I&EC research
Industrial & Engineering Chemistry Research

Article

pubs.acs.org/IECR

Synthesis and Properties of Organic–Inorganic Hybrid Materials Based on Glycerol

Ignacio E. dell'Erba, Cristina E. Hoppe, and Roberto J. J. Williams*

Institute of Materials Science and Technology (INTEMA), University of Mar del Plata and National Research Council (CONICET), J. B. Justo 4302, 7600 Mar del Plata, Argentina

ABSTRACT: The great supply of glycerol as a byproduct of the production of biodiesel has motivated interest in its use in new applications. In this study, we report the synthesis and properties of organic–inorganic hybrid materials based on glycerol. Glycerol (Gly) was reacted with 3-isocyanatopropyltriethoxysilane (IPTES) in the presence of dibutyltin dilaurate (DBTDL) as a catalyst, using a molar ratio (r = IPTES/Gly) between 0.75 and 3. The sol–gel polycondensation of the resulting precursors in the presence of a formic acid solution led to transparent solid materials with a biphasic structure consisting of glycerol-rich domains dispersed in the organic–inorganic hybrid matrix. An increase in the r value changed the hybrid materials from hydrophilic to hydrophobic. The contact angle of water droplets varied from 43.6° for r = 0.75 to 95.1° for r = 3. Each of the materials exhibited a broad glass-to-rubber transition, with the maximum of the damping peak located in the 54–70 °C range. The relatively intense tan δ peaks of the hybrid materials suggest their possible use in devices requiring vibrational damping. The maximum damping capacity corresponded to the hybrid with r = 1.5, which exhibited a loss area LA (area under the loss modulus peak) of 13.5 GPa·K. High values of the rubbery modulus were observed, varying from 130 MPa for r = 0.75 to 720 MPa for r = 3. Values of the glassy modulus were also high, and the maximum value was observed for the hybrid with r = 1.5. The hybrid materials could also be colored through the incorporation of a very small amount of functionalized gold nanoparticles.

1. INTRODUCTION

In recent years, the increasing low-cost supply of glycerol from the production of biodiesel has led to interest in its use in new applications. Examples are the use of glycerol as the carbon source for fermentation processes[1] or hydrogen generation;[2,3] its transformation into products with added value through chlorination[4] and transesterification;[5] and its conversion to succinic acid,[6] tertiary butyl ethers,[7] polyhydric alcohols,[8] and new additives for diesel fuels.[9,10] In addition, glycerol has been employed for the development of advanced materials such as hyperbranched polyglycerol derivatives[11,12] and poly(glycerol sebacate), which is used in biomedical applications.[13−16] Another approach is to add value to traditional products based on glycerol. For example, properties of conventional glycerol-derived alkyd resins can be improved through the addition of layered silicates.[17]

Glycerol can also be used to modify organic–inorganic hybrid materials obtained by conventional sol–gel reactions. Adding glycerol to tri- and tetraalkoxysilane precursors produces covalent bonding in the hybrid network through C–O–Si bonds. Depending on the amount of glycerol and the reaction conditions, clusters of unreacted glycerol can be present as dispersed domains in the resulting hybrid material.[18] The fact that glycerol is a biocompatible molecule exhibiting osmoprotective properties has promoted its incorporation as a modifier of silica gels used in the encapsulation of living cells.[19−21] This reduces the inorganic network densification and the mechanical constraints on the cells while simultaneously providing a more biocompatible interface. Both effects increase the fraction of encapsulated cells that remain alive in the hybrid material.[21]

A different strategy for incorporating glycerol into organic–inorganic hybrid materials is to react it with a stoichiometric amount of an isocyanate containing alkoxysilane groups such as 3-isocyanatopropyltriethoxysilane (IPTES). This converts the glycerol molecule into a triurethane containing nine ethoxysilane groups in its structure. This precursor can be incorporated into an organic–inorganic hybrid network through conventional sol–gel chemistry. Wilkes and coworkers synthesized abrasion-resistant hybrid coatings using a precursor derived from the reaction of glycerol with IPTES blended with a variety of metal alkoxides.[22,23] Unlike these earlier reports that considered blends of different alkoxides to generate the desired abrasion resistance, in this study, we focused on the properties of hybrids derived from the sol–gel polycondensation of the neat precursor obtained by reaction of glycerol with IPTES. The variable of interest was the initial molar ratio of the two components (r = IPTES/Gly), which ranged between r = 0.75 and r = 3 (stoichiometric value). The use of a deficit of IPTES with respect to glycerol enabled the synthesis of hybrid materials with a set of properties that could be useful for different applications.

2. EXPERIMENTAL METHODS

2.1. Synthesis of Precursors. Anhydrous glycerol (Gly, ACS 98–100%, Cicarelli) was mixed with 3-isocyanatopropyltriethoxysilane (IPTES, >95%, Fluka) in molar ratios (r = IPTES/Gly) of 0.75, 1, 1.5, or 3. Dibutyltin dilaurate (DBTDL,

Received: February 13, 2012
Revised: May 8, 2012
Accepted: May 18, 2012
Published: May 18, 2012

dx.doi.org/10.1021/ie300393n | Ind. Eng. Chem. Res. 2012, 51, 7793–7799

95%, Aldrich) was added as a catalyst in a proportion of 0.5 wt % with respect to IPTES. The reaction was carried out in closed flasks with stirring at 50 °C for 3 h.

2.2. Synthesis of Hybrid Networks. A formic acid solution (pH 4) was added to the precursor in the necessary amount to obtain a molar ratio of H_2O/Si−OEt = 1. The solution was vigorously stirred for 5 min and then transferred to an open Teflon mold placed in an oven. The sol−gel reaction was allowed to proceed for 24 h at 40 °C, for 24 h at 80 °C, and for 2 h at 110 °C.

2.3. Synthesis of Colored Hybrid Networks. Au nanoparticles (NPs) with an average size of 1.5 nm, coated with 6-mercapto-1-hexanol, were synthesized by the procedure described by Tan et al.[24] Terminal OH groups of the organic ligands were reacted with a slight excess of IPTES, using a mixed solvent composed of tetrahydrofuran (THF) and dimethylformamide (DMF) (80:20 by volume). DBTDL was used as a catalyst (0.5 wt % with respect to IPTES). The reaction was carried out at room temperature for 3 h. NPs were precipitated and washed three times with cyclohexane to remove residual IPTES. They were stored as stable dispersions in DMF.

The precursor synthesized with r = 1.5 was mixed with the DMF solution of Si(OEt)$_3$-functionalized Au NPs in a proportion such that the concentration of Au NPs in the precursor was 0.05 wt %. The hybrid network was synthesized following the procedure described in the previous subsection, except for the cure cycle, which was carried out at 50 °C for 72 h. The prolonged cure at 50 °C was employed to ensure the elimination of volatiles in the absence of postcure steps at higher temperatures.

2.4. Techniques. Fourier transform infrared (FTIR) spectra of the precursors were obtained with a Mattson Genesis II spectrometer employing coatings on NaCl windows. FTIR spectra of the hybrid networks were obtained with a Nicolet 6700 spectrometer in ATR (attenuated total reflectance) mode using a smart Orbit ATR accessory with a diamond crystal. Spectra of Si(OEt)$_3$-functionalized Au NPs were recorded with the Nicolet 6700 spectrometer in transmission mode, including samples in pellets of spectroscopic-grade KBr. In all cases, the resolution was 2 cm^{-1}, and the spectra were averaged over 32 scans. Images of the morphology of the hybrid networks were obtained with a video camera (Leica DC 100) coupled to a transmission optical microscope (Leica DMLB microscope), with and without crossed polarizers. A contact angle goniometer (model 500 from Ramé-Hart Instruments with DROPimage Advanced Software) was employed to determine the contact angles of drops (5 μL) of twice-distilled water at room temperature by the sessile drop method. Water drops were placed manually with a micropipet, and contact angle measurements were performed 30−60 s after placement of the drop using the circle method included in the software of the instrument. At least four drops were measured for each sample. Dynamic mechanical spectra of hybrid networks were obtained with a Perkin-Elmer DMA-7 instrument operating at 1 Hz in the three-point bending mode. The temperature range was between −75 and 150 °C, and the heating rate was 10 °C/min. Specimens with the following dimensions were used: length = 20 mm (span = 15 mm), width = 5 mm, and thickness = 1 mm.

3. RESULTS AND DISCUSSION

3.1. Precursors. Figure 1 shows the reaction of glycerol with IPTES for r = 3 (stoichiometric ratio), leading to a

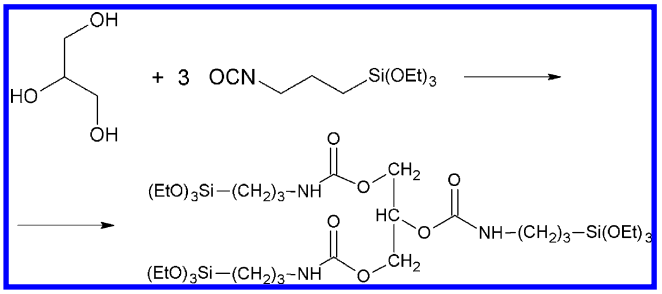

Figure 1. Precursor generated by reaction of glycerol with a stoichiometric amount of IPTES (r = 3).

precursor with nine Si−OEt groups. The use of a deficit of IPTES (r < 3) leads to a distribution of precursors with different numbers of Si−OEt groups per molecule. The fraction of unreacted OH groups at full conversion of IPTES is equal to $(1 - r/3)$. The fraction of unreacted glycerol can be estimated by assuming equal reactivity of the three OH groups toward IPTES. This gives a residual fraction of glycerol equal to $(1 - r/3)^3$. This fraction is obviously zero for the stoichiometric formulation and reaches a value of 42.2% for the precursor synthesized with r = 0.75.

The advance in the reaction of IPTES with glycerol was followed by the intensity of the NCO peak at 2276 cm^{-1} in FTIR spectra. Complete disappearance of this peak was observed after 3 h at 50 °C for all of the precursors synthesized with different values of the molar ratio (r). As an example, Figure 2a shows the initial FTIR spectrum of the formulation with r = 1.5. An intense peak characteristic of the NCO group is observed at 2276 cm^{-1}. In Figure 2b, this peak has completely disappeared after 3 h reaction at 50 °C, whereas a characteristic

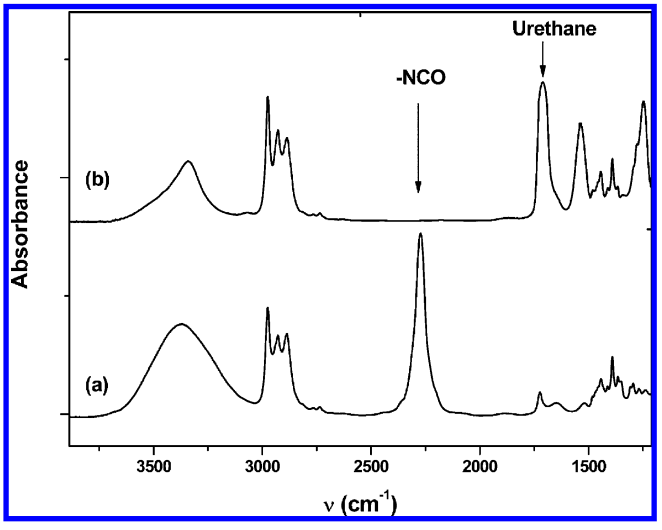

Figure 2. FTIR spectra recorded for the precursor synthesized with r = 1.5: (a) initial formulation showing the characteristic peak of isocyanate at 2276 cm^{-1} and (b) precursor obtained after 3 h at 50 °C, showing the disappearance of the isocyanate peak and the appearance of a characteristic peak of the urethane group. Spectra were recorded at room temperature.

dx.doi.org/10.1021/ie300393n | Ind. Eng. Chem. Res. 2012, 51, 7793−7799

peak of the generated urethane group appears in the spectrum. (Spectra were recorded at room temperature.)

3.2. Hybrid Networks. A chemically cross-linked network is produced by hydrolysis and condensation of Si−OEt groups leading to Si−O−Si chemical bonds (sol−gel chemistry). A variety of acid and basic catalysts can be used for this purpose. In our case, we used a formic acid solution that leads to fast hydrolysis and partial condensation, producing a network with a fraction of uncondensed SiOH groups.[25,26] The advantage of using formic acid is that the residual catalyst and the volatiles produced in the reaction (ethanol, ethyl formate) can be easily eliminated. The fraction of uncondensed SiOH groups can be varied by the thermal cycle used in the sol−gel reaction.

Figure 3 shows FTIR spectra of the precursor and the hybrid material resulting from the sol−gel process for r = 1.5. The

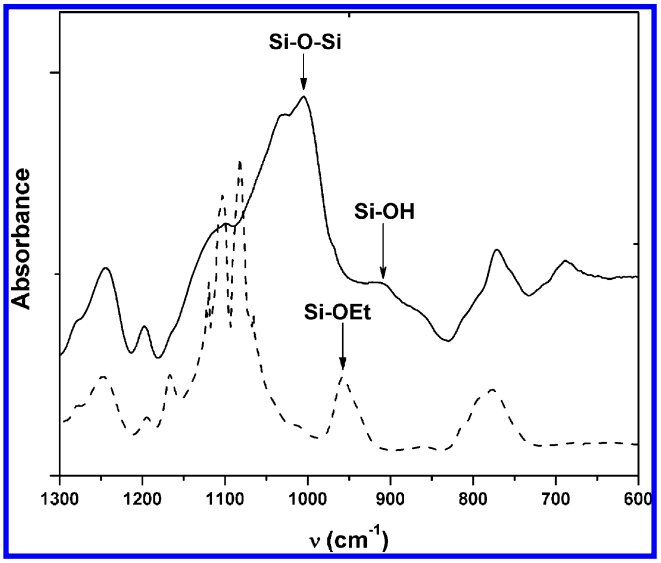

Figure 3. FTIR spectra of the hybrid network generated after the sol−gel process (solid line) and the precursor (dashed line) for r = 1.5. The characteristic band of the Si−OEt group at 958 cm^{-1} is not discernible in the spectrum of the hybrid material. In turn, new bands that are characteristic of Si(OH) groups, at about 920 cm^{-1}, and Si−O−Si bonds, in the 1000−1050 cm^{-1} region, appear in the spectrum of the hybrid material.

characteristic Si−OEt peak at 958 cm^{-1},[26] present in the spectrum of the precursor, can not be observed in the spectrum of the hybrid network, meaning that hydrolysis of Si−OEt groups was almost complete. The broad band in the range 1000−1050 cm^{-1} is characteristic of Si−O−Si bonds, whereas the small peak close to 920 cm^{-1} reveals the presence of uncondensed SiOH groups.[26]

All hybrid materials were transparent (Figure 4). At room temperature, the hybrid with r = 0.75 was a relatively soft material, whereas those synthesized with r values in the range of 1−3 were glasses. The glass with r = 3 was rather brittle, whereas those with r = 1 and 1.5 could be easily machined.

As discussed in section 3.1, materials obtained from precursors synthesized with a stoichiometric ratio r < 3 include a fraction of free glycerol. For a particular hybrid material, it was reported that, at concentrations higher than 4%, glycerol was present as dispersed domains.[18] Based on this observation, we examined the morphology of the hybrid materials by transmission optical microscopy (TOM). Each hybrid material with r < 3 showed a biphasic morphology. As an example,

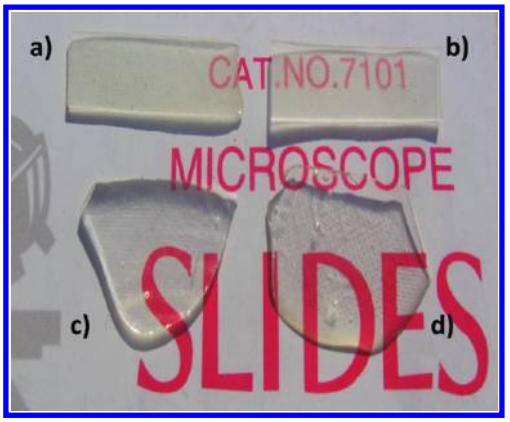

Figure 4. Photographs of the hybrid materials synthesized using different initial stoichiometries (r): r = (a) 0.75, (b) 1, (c) 1.5, and (d) 3.

Figure 5 shows TOM images of hybrids synthesized with r = 1 and r = 1.5. The dispersed domains are assigned to free glycerol (eventually including low-molar-mass species not connected to the hybrid network). The fraction of free glycerol in the

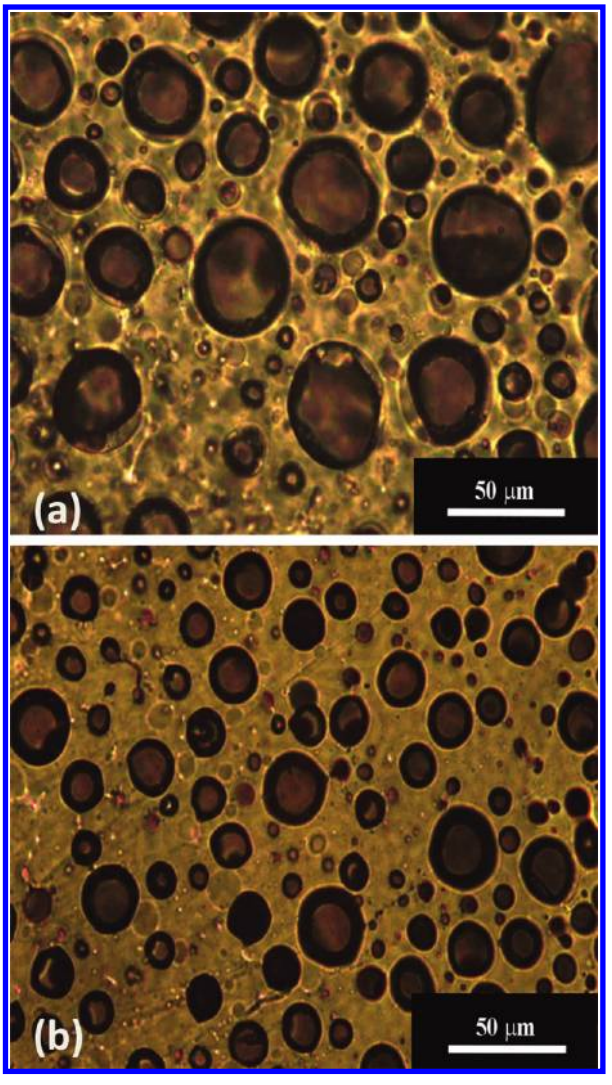

Figure 5. Transmission optical microscopy (TOM) images of hybrids synthesized with r = (a) 1 and (b) 1.5.

dx.doi.org/10.1021/ie300393n | Ind. Eng. Chem. Res. 2012, 51, 7793−7799

precursors was estimated as 29.6% for r = 1 and 12.5% for r = 1.5 (see section 3.1). It is interesting to observe that the size of the dispersed domains decreased when r was increased from 1 to 1.5 (Figure 5). Moreover, for r = 3, dispersed domains were no longer observed. The transparency of the hybrid materials despite their biphasic nature can be attributed to the matching of the refractive indices of the two phases.

To assess possible applications of the hybrid materials, different properties were determined. The results are summarized in Table 1 and discussed in the remainder of this section. Because of their transparency and smooth surface, these materials could be used as coatings, in which case characterization of their hydrophobic character is important. Figure 6 shows images of water drops deposited on the surfaces of hybrids with r = 0.75, 1, 1.5, and 3. A significant variation of the contact angle with the stoichiometric ratio was observed (Table 1). The contact angles varied from 43.6° for r = 0.75 to 95.1° for r = 3. Therefore, an increase in the r value changed the hybrid materials from hydrophilic to hydrophobic. This is obviously the consequence of decreasing the fraction of residual OH groups as they were increasingly converted to urethane moieties.

Table 1. Properties of Hybrid Materials Derived from Precursors Synthesized with Different Molar Stoichiometric Ratios (r = IPTES/Gly)

	r = 0.75	r = 1	r = 1.5	r = 3
contact angle of water (deg)	43.6	67.0	92.7	95.1
elastic modulus at −65 °C (GPa)	2.80	5.11	5.68	3.89
elastic modulus at 120 °C (GPa)	0.13	0.35	0.68	0.72
area under loss modulus peak (GPa·K)	0.4	9.5	13.5	4.2

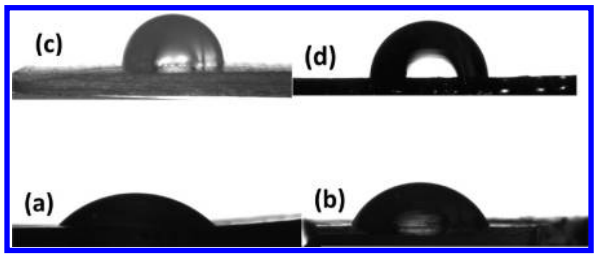

Figure 6. Images of water droplets deposited on the surface of hybrids with r = (a) 0.75, (b) 1, (c) 1.5, and (d) 3.

Dynamical mechanical characterization was also performed for the set of hybrid materials. Figure 7 shows the storage moduli and damping (tan δ) peaks of the different hybrids in the temperature range extending from about −75 to 150 °C. Each of the materials exhibited a broad glass-to-rubber transition, with the maximum of the damping peak located in the 54−70 °C range. The hybrid with r = 0.75 showed a second damping peak at −43 °C, much sharper than that located at higher temperatures. Characteristic values of the elastic modulus in the glassy and rubbery states are reported in Table 1. High values of the rubbery modulus were observed, varying from 130 MPa for r = 0.75 to 720 MPa for r = 3. The increase of the rubbery modulus with the stoichiometric ratio r is explained by the corresponding increase in the cross-link density of the hybrid materials. Values of the glassy modulus were also high, but in this case, the maximum value was observed for the hybrid with r = 1.5. This might be because the matrix has a higher elastic modulus than the dispersed domains (explaining the increase of the modulus from r = 0.75 to r = 1.5), but the cohesive energy density of the matrix decreases with decreasing fraction of OH groups (explaining the decrease of the modulus from r = 1.5 to r = 3). The cohesive energy density and active subglass relaxations are the main factors determining the value of the glass transition temperature of a glassy polymer.[27] For most cross-linked polymers, the elastic modulus in the rubbery state is 100−1000 times smaller than the modulus in the glassy state. Because of the high values of the rubbery modulus, the glycerol-based hybrid materials showed a much smaller decrease of the elastic modulus along the glass transition. For the sample with r = 3, the elastic modulus decreased by only a factor of 5.4 along the glass transition.

The relatively intense tan δ peaks of the hybrid materials suggest the possible use of these materials in devices requiring vibrational damping.[28,29] The damping capacity of a material can be quantified in terms of the loss area (LA), defined as the integral of the loss modulus as a function of temperature (area under the loss modulus peak).[30] Figure 8 shows the loss modulus as a function of temperature for the hybrid with r = 1.5, and Table 1 lists the LA values for all samples. The maximum damping capacity corresponded to the hybrid with r = 1.5, which exhibited an LA value of 13.5 GPa·K. This is in the range of values reported for acrylic-, methacrylic-, styrenic-, and butadiene-based copolymers exhibiting damping properties.[30]

3.3. Colored Hybrid Networks. Coloring the hybrid coatings might be useful for decorative purposes. Gold nanoparticles (NPs) were used because of their high extinction coefficients and the stability of the resulting composites. A first attempt was performed with Au NPs coated with 6-mercapto-1-hexanol, synthesized according to the procedure described by Tan et al.[23] The presence of a terminal OH group in the organic ligands enabled the NPs to be correctly dispersed in the precursor of the hybrid material. However, a polymerization-induced phase separation (PIPS) of NPs took place in the course of the sol−gel reaction, leading to the formation of agglomerates of Au NPs. The PIPS of NPs initially dispersed in monomers has been theoretically predicted.[31] To avoid phase separation of NPs, it is necessary to produce the covalent bonding of the organic ligands to the polymeric matrix.[32] For this purpose, terminal OH groups were reacted with IPTES to introduce $Si(OEt)_3$ groups into the coating of Au NPs. Figure 9 shows an FTIR spectrum of the Au NPs coated with ligands functionalized with $Si(OEt)_3$ groups. The spectrum shows a Si−O−C asymmetric stretching band at 1104 cm^{-1}, the characteristic Si−OEt band at 958 cm^{-1}, and a C═O stretching band at 1633 cm^{-1}, assigned to urethane groups. The presence of a residual band at 3400 cm^{-1} reveals that only a partial conversion of OH into urethane groups occurred. The absence of the isocyanate peak at 2276 cm^{-1} indicates that unreacted IPTES was effectively removed by washing with cyclohexane.

The functionalization of Au NPs with $Si(OEt)_3$ groups enabled their covalent bonding to the cross-linked network. In this case, aggregates were not formed, and the NPs retained their original size.[32] Figure 10 compares photographs of films (1-mm thickness) obtained from the hybrid material with r = 1.5, without Au NPs (Figure 10a) and with 0.05 wt % Au NPs (Figure 10b). The presence of a very small amount of Au NPs produced a reddish brown coloration of the material.

dx.doi.org/10.1021/ie300393n | Ind. Eng. Chem. Res. 2012, 51, 7793−7799

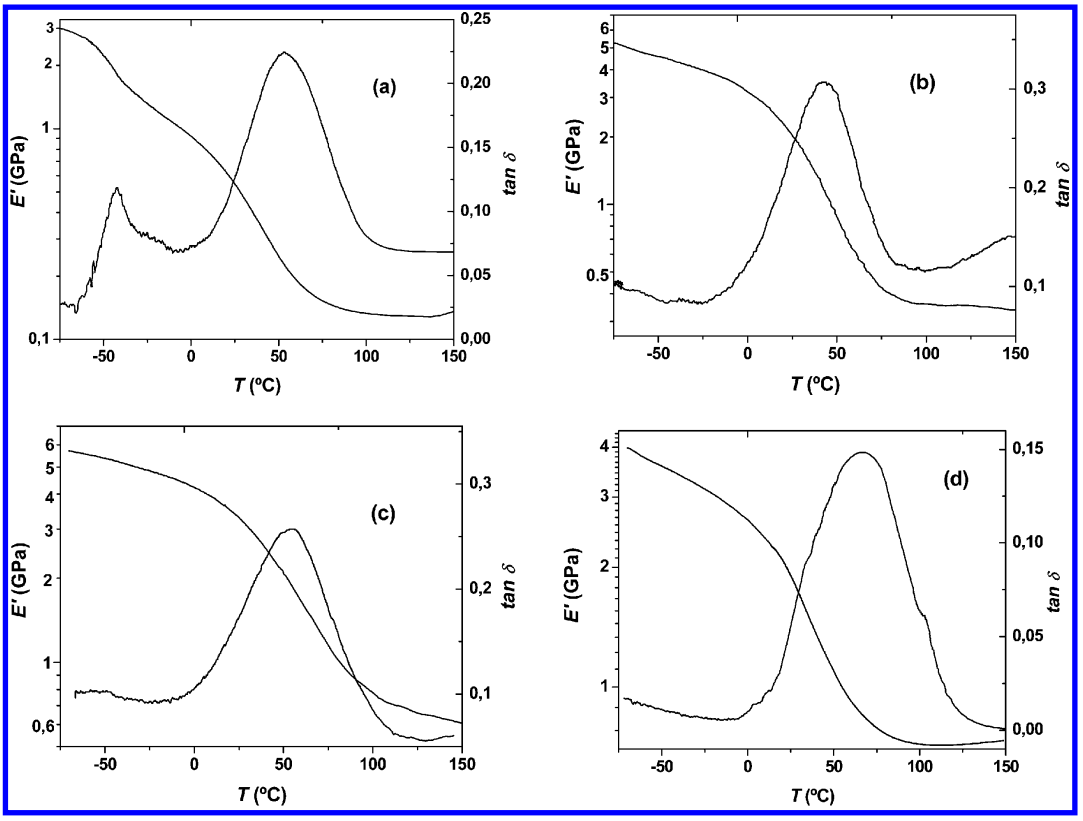

Figure 7. Storage modulus (E') and damping peak (tan δ) for the set of hybrids with r = (a) 0.75, (b) 1, (c) 1.5, and (d) 3.

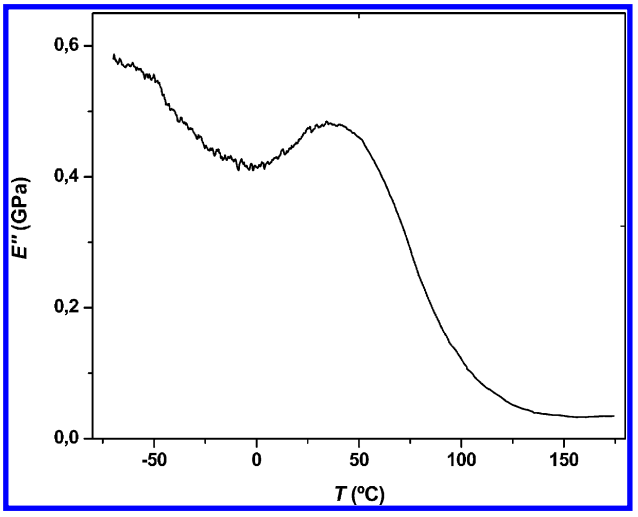

Figure 8. Loss modulus (E'') as a function of temperature for the hybrid with r = 1.5.

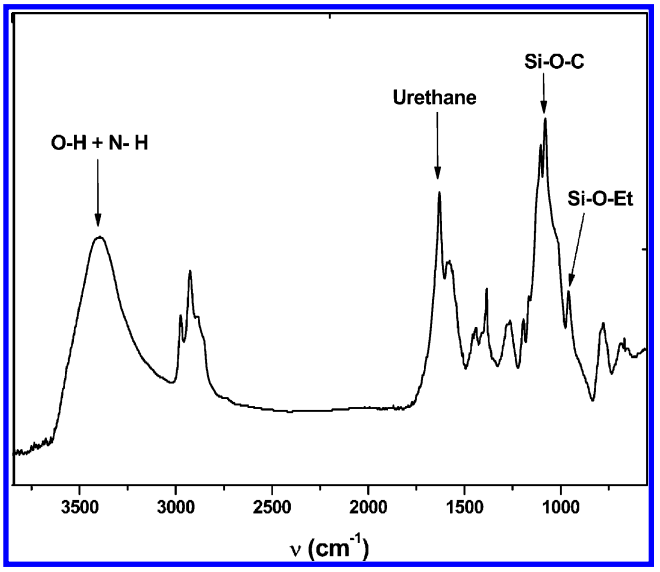

Figure 9. FTIR spectrum of Au NPs functionalized with organic ligands containing terminal $Si(OEt)_3$ groups.

4. CONCLUSIONS

Organic−inorganic hybrid materials were obtained by the sol−gel polycondensation of a precursor obtained by reaction of glycerol (Gly) with 3-isocyanatopropyltriethoxysilane (IPTES). The variable of interest was the initial molar ratio of the two components (r = IPTES/Gly), which ranged between r = 0.75 and r = 3 (stoichiometric value). The use of a deficit of IPTES with respect to glycerol enabled the synthesis of hybrid materials with a broad set of useful properties for practical applications. The materials were transparent, but they could easily be colored using conveniently functionalized Au NPs. An increase in the r value changed the materials from hydrophilic to hydrophobic. The contact angle of water droplets varied from 43.6° for r = 0.75 to 95.1° for r = 3. Each of the materials exhibited a broad glass-to-rubber transition, with the maximum of the damping peak located in the 54−70 °C range. The relatively intense tan δ peaks of the hybrid materials suggest their possible use in devices requiring vibrational damping. The maximum damping capacity corresponded to the hybrid with r = 1.5, which exhibited an LA value of 13.5 GPa·K. High values of the rubbery modulus were observed, varying from 130 MPa for r = 0.75 to 720 MPa for r = 3. Values of the glassy modulus

dx.doi.org/10.1021/ie300393n | Ind. Eng. Chem. Res. 2012, 51, 7793−7799

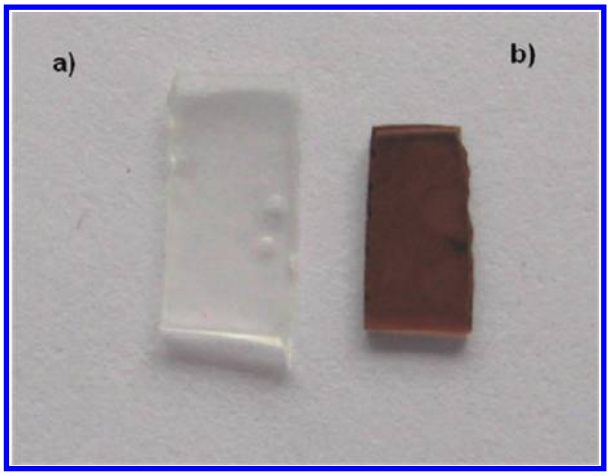

Figure 10. Photographs of films of hybrid materials (1-mm thickness) synthesized from precursors with r = 1.5: (a) neat hybrid material, (b) hybrid material containing 0.05 wt % Au NPs.

were also high, and the maximum value was observed for the hybrid with r = 1.5.

AUTHOR INFORMATION

Corresponding Author

*Tel.: +54-223-4816600. Fax: +54-223-4810046. E-mail: williams@fi.mdp.edu.ar.

Notes

The authors declare no competing financial interest.

ACKNOWLEDGMENTS

The authors acknowledge the financial support of the University of Mar del Plata, the National Research Council (CONICET), and the National Agency for the Promotion of Science and Technology (ANPCyT), Argentina.

REFERENCES

(1) Çelik, E.; Ozbay, N.; Oktar, N.; Çalik, P. Use of Biodiesel Byproduct Crude Glycerol as the Carbon Source for Fermentation Processes by Recombinant *Pichia pastoris*. *Ind. Eng. Chem. Res.* **2008**, *47*, 2985.

(2) Ghosh, D.; Sobro, I. F.; Hallenbeck, P. C. Stoichiometric Conversion of Biodiesel Derived Crude Glycerol to Hydrogen: Response Surface Methodology Study of the Effects of Light Intensity and Crude Glycerol and Glutamate Concentration. *Bioresour. Technol.* **2012**, *106*, 154.

(3) Nichele, V.; Signoretto, M.; Menegazzo, F.; Gallo, A.; Dal Santo, V.; Cruciani, G.; Cerrato, G. Glycerol Steam Reforming for Hydrogen Production: Design of Ni Supported Catalysts. *Appl. Catal. B: Environ.* **2012**, *111−112*, 225.

(4) Santacesaria, E.; Tesser, R.; Di Serio, M.; Casale, L.; Verde, D. New Process for Producing Epichlorohydrin via Glycerol Chlorination. *Ind. Eng. Chem. Res.* **2010**, *49*, 964.

(5) Morales, G; Paniagua, M.; Melero, J. A.; Vicente, G.; Ochoa, C. Sulfonic Acid-Functionalized Catalysts for the Valorization of Glycerol via Transesterification with Methyl Acetate. *Ind. Eng. Chem. Res.* **2011**, *50*, 5898.

(6) Vlysidis, A.; Binns, M.; Webb, C.; Theodoropoulos, C. Glycerol Utilisation for the Production of Chemicals: Conversion to Succinic Acid, a Combined Experimental and Computational Study. *Biochem. Eng J.* **2011**, *58−59*, 1.

(7) Cheng, J. K.; Lee, C. L.; Jhuang, Y. T.; Ward, J. D.; Chien, I. L. Design and Control of the Glycerol Tertiary Butyl Ethers Process for the Utilization of a Renewable Resource. *Ind. Eng. Chem. Res.* **2011**, *50*, 12706.

(8) Maglinao, R. L.; He, B. B. Catalytic Thermochemical Conversion of Glycerol to Simple and Polyhydric Alcohols Using Raney Nickel Catalysts. *Ind. Eng. Chem. Res.* **2011**, *50*, 6028.

(9) Chang, J. S.; Lee, Y. D.; Chou, L. C. S.; Ling, T. R.; Chou, T. C. Methylation of Glycerol with Dimethyl Sulfate to Produce a New Oxygenate Additive for Diesels. *Ind. Eng. Chem. Res.* **2012**, *51*, 655.

(10) Hernández, D.; Fernández, J. J.; Mondragón, F.; López, D. Production and Utilization Performance of a Glycerol Derived Additive for Diesel Engines. *Fuel* **2012**, *92*, 130.

(11) Fischer, W.; Quadir, M. A.; Barnard, A.; Smith, D. K.; Haag, R. Controlled Release of DNA from Photoresponsive Hyperbranched Polyglycerols with Oligoamine Shells. *Macromol. Biosci.* **2011**, *11*, 1736.

(12) Cuggino, J. C.; Alvarez, I, C. I.; Strumia, M. C.; Welker, P.; Licha, K.; Steinhilber, D.; Mutihac, R. C.; Calderón, M. Thermosensitive Nanogels Based on Dendritic Polyglycerol and *N*-Isopropylacrylamide for Biomedical Applications. *Soft Matter* **2011**, *7*, 11259.

(13) Chen, Q. Z.; Ishii, H.; Thouas, G. A.; Lyon, A. R.; Wright, J. S.; Blaker, J. J.; Chrzanowski, W.; Boccaccini, A. R.; Alj, N. N.; Knowles, J. C.; Harding, S. E. An Elastomeric Patch Derived from Poly(glycerol sebacate) for Delivery of Embryonic Stem Cells to the Heart. *Biomaterials* **2010**, *31*, 3885.

(14) Liang, S. L.; Cook, W. D.; Thouas, G. A.; Chen, Q. Z. The Mechanical Characteristics and *In Vitro* Biocompatibility of Poly-(glycerol sebacate)/Bioglass® Elastomeric Composites. *Biomaterials* **2010**, *31*, 8516.

(15) Liang, S. L.; Cook, W. D.; Chen, Q. Z. Physical Characterization of Poly(glycerol sebacate)/Bioglass® Composites. *Polym. Int.* **2012**, *61*, 17.

(16) Sant, S.; Hwang, C. M.; Lee, S. H.; Khademhosseini, A. Hybrid PGS-PCL microfibrous scaffolds with improved mechanical and biological properties. *J. Tissue Eng. Regen. Med.* **2011**, *5*, 283.

(17) Lin, G.; Zhang, X.; Li, Y.; Allen, W.; Noda, I.; Mark, J. E. Some Nanocomposites Based on a Glycerol-Derived Alkyd Resin and Layered Silicates. *Mol. Cryst. Liq. Cryst.* **2008**, *483*, 33.

(18) Haruvy, Y.; Ryabov, Y.; Arkhipov, V.; Gutina, A.; Axelrod, E.; Feldman, Y. Fast-Sol−Gel Derived Silsesquioxane Glasses Embodying Glycerol Moieties: Dielectric Properties and Morphology. *J. Non-Cryst. Solids* **2002**, *305*, 226.

(19) Gill, I.; Ballesteros, A. Encapsulation of Biologicals within Silicate, Siloxane, and Hybrid Sol−Gel Polymers: An Efficient and Generic Approach. *J. Am. Chem. Soc.* **1998**, *120*, 8587.

(20) Harper, J. C.; Lopez, D. M.; Larkin, E. C.; Economides, M. K.; McIntyre, S. K.; Alam, T. M.; Tartis, M. S.; Werner-Washburne, M.; Brinker, C. J.; Brozik, S. M.; Wheeler, D. R. Encapsulation of *S. cerevisiae* in Poly(glycerol) Silicate Derived Matrices: Effect of Matrix Additives and Cell Metabolic Phase on Long-Term Viability and Rate of Gene Expression. *Chem. Mater.* **2011**, *23*, 2555.

(21) Avnir, D.; Coradin, T.; Lev, O.; Livage, J. Recent Bio-Applications of Sol−Gel Materials. *J. Mater. Chem.* **2006**, *16*, 1013.

(22) Wen, J.; Vasudevan, V. J.; Wilkes, G. L. Abrasion Resistant Inorganic/Organic Coating Materials Prepared by the Sol−Gel Method. *J. Sol−Gel Sci. Technol.* **1995**, *5*, 115.

(23) Wen, J.; Wilkes, G. L. Synthesis and Characterization of Abrasion Resistant Coating Materials Prepared by the Sol−Gel Approach. I. Coatings Based on Functionalized Aliphatic Diols and Diethylenetriamine. *J. Inorg. Org. Polym.* **1995**, *5*, 343.

(24) Tan, H.; Zhan, T.; Fan, W. Y. Direct Functionalization of the Hydroxyl Group of the 6-Mercapto-1-hexanol (MCH) Ligand Attached to Gold Nanoclusters. *J. Phys. Chem. B* **2006**, *110*, 21690.

(25) Eisenberg, P.; Erra-Balsells, R.; Ishikawa, Y.; Lucas, J. C.; Nonami, H.; Williams, R. J. J. Silsesquioxanes Derived from the Bulk Polycondensation of 3-(Methacryloxypropyl)trimethoxysilane with Concentrated Formic Acid: Evolution of Molar Mass Distributions and Fraction of Intramolecular Cycles. *Macromolecules* **2002**, *35*, 1160.

(26) dell'Erba, I. E.; Fasce, D. P.; Williams, R. J. J.; Erra-Balsells, R.; Fukuyama, Y.; Nonami, H. Poly(silsesquioxanes) Derived from the Hydrolytic Condensation of Organotrialkoxysilanes Containing Hydroxyl Groups. *J. Organomet. Chem.* **2003**, *686*, 42.

(27) Pascault, J. P.; Sautereau, H.; Verdu, J.; Williams, R. J. J. *Thermosetting Polymers*; Marcel Dekker: New York, 2002; p 282.
(28) Liang, F.; Gou, J.; Kapat, J.; Gu, H.; Song, G. Multifunctional Nanocomposite Coating for Wind Turbine Blades. *Int. J. Smart Nano Mater.* **2011**, *2*, 120.
(29) Kurano, S. Experimental Study on the Effect of Elastomer Coating on the Vibration-Damping Property of Steel and CFRP Plates for Ship's Hull. *Trans. Jpn. Soc. Mech. Eng. A* **2005**, *71*, 982.
(30) Fay, J. J.; Murphy, C. J.; Thomas, D. A.; Sperling, L. H. Effect of Morphology, Crosslink Density and Miscibility on Interpenetrating Polymer Network Damping Effectiveness. *Polym. Eng. Sci.* **1991**, *31*, 1731.
(31) Soulé, E. R.; Borrajo, J.; Williams, R. J. J. Thermodynamic Analysis of a Polymerization-Induced Phase Separation in Nanoparticle−Monomer−Polymer Blends. *Macromolecules* **2007**, *40*, 8082.
(32) dell'Erba, I. E.; Hoppe, C. E.; Williams, R. J. J. Synthesis of Silver Nanoparticles Coated with OH-Functionalized Organic Groups: Dispersion and Covalent Bonding in Epoxy Networks. *Langmuir* **2010**, *26*, 2042.